



Cellular and biomolecular detection based on suspended microchannel resonators

Juhee Ko¹ · Jaewoo Jeong¹ · Sukbom Son¹ · Jungchul Lee¹

Received: 29 June 2021 / Revised: 23 August 2021 / Accepted: 3 September 2021 / Published online: 12 September 2021
© Korean Society of Medical and Biological Engineering 2021

Abstract

Suspended microchannel resonators (SMRs) have been developed to measure the buoyant mass of single micro-/nanoparticles and cells suspended in a liquid. They have significantly improved the mass resolution with the aid of vacuum packaging and also increased measurement throughput by fast resonance frequency tracking while target objects travel through the microchannel without stopping or even slowing down. Since their invention, various biological applications have been enabled, including simultaneous measurements of cell growth and cell cycle progression, and measurements of disease associated physicochemical change, to name a few. Extension and advancement towards other promising applications with SMRs are continuously ongoing by adding multiple functionalities or incorporating other complementary analytical metrologies. In this paper, we will thoroughly review the development history, basic and advanced operations, and key applications of SMRs to introduce them to researchers working in biological and biomedical sciences who mostly rely on classical and conventional methodologies. We will also provide future perspectives and projections for SMR technologies.

Keywords Buoyant mass · Cellular and biomolecular detection · Disease diagnosis · Growth rate · Suspended microchannel resonators (SMRs)

1 Introduction

Many biological systems naturally exist in a non-uniform state. Thus, different cells from the same cell population may have dissimilar functions and states depending on some environmental and intrinsic factors. Early cell studies mainly focused on group analysis using quantitative phase microscopy [1–4] or gradient centrifugation [5, 6], ignoring different characteristics of each individual cell. From a biological standpoint of view, properties and behaviors of each individual cell are often more valuable than those of the entire population. For example, in the case of cancer cells, important characteristics such as resistance to therapeutic treatment may occur in outliers which group analyses tend to ignore [7, 8]. In short, aforementioned ensemble methods bear intrinsic limitations to some degree considering the context of biological measurements.

Therefore, a scrutiny of intricate discrepancies within the cell population at a specific state has become essential not only for disease diagnosis but also for fundamental understanding of cells. Coulter counter and flow cytometry were the representative methodologies for single cell measurement and analysis to fulfill such needs [9, 10]. These technologies could obtain both group and individual properties from size and volume characterization of suspended cells. Meanwhile, mass as a measurement parameter, which is determined by intracellular water, proteins, carbohydrates, lipids, etc., is used to monitor cellular activities more effectively such as metabolism or proliferation [11, 12]. For this reason, mass-based single cell analysis using MEMS resonator was proposed. Measurement of cell mass change using a resonator allows for observation of biophysical activities, such as suppressed growth of virus-infected animal cells [13]. However, due to the nature of acceptable cell habitats, the resonator must be placed in a fluidic environment throughout the experiment. Such a requirement increases the dissipation of vibration energy and correspondingly decreases the mass sensitivity. This sensitivity reduction is detrimental to the purpose of cell diagnosis, where cells outside the normal range must be precisely identified.

✉ Jungchul Lee
jungchullee@kaist.ac.kr

¹ Department of Mechanical Engineering, Korea Advanced Institute of Science and Technology (KAIST), Daehak-ro 291, Daejeon, South Korea

In 2003, a novel platform called suspended microchannel resonator (SMR) was developed to increase the mass sensitivity by incorporating both the target sample and its preferred fluidic environment inside the resonator [14, 15]. Compared to previous approaches relying on solid resonators, measurement of resonance frequency shifts with SMRs enables highly sensitive monitoring, thus allowing an improved cell classification performance. This method also enables easier sample control and faster measurement than previous methods where single cells are manually loaded and measured on resonators. Since its first introduction, SMR technologies have continuously developed, significantly surpassing previous methods with the advantage of high throughput measurement. Likewise, researches in disease diagnosis and individual cell analysis are also accelerating based on the present SMR technology. Nowadays, SMR is playing an active role in various important biomedical fields, such as monitoring the circulating tumor cells [16] or cancer cells during drug injection [17].

In this review, we briefly introduce fabrication and operation methods of SMRs and focus on applications associated with cellular and biomolecular detection. First, the history of the channel resonator fabrication will be explained, followed by the basic operation method for actuating/detecting the SMR and detailed operation methods for bio-applications. In the biomedical detection section, we will discuss their implications for diverse biomedical applications with the various measurement parameters such as buoyant mass, stiffness, and so on. We also include near future perspectives towards multi-modal measurements with functional element integrated SMR systems or currently existing SMR setups combined with other analytical instruments. We envisage this review to broaden the scope of potential SMR applications in cellular and biomolecular detection fields.

2 Development history

3 Methods

Starting with a hydrometer that measures the buoyancy of fluids in a hollow tube, hollow structure devices were first used in measuring fluid density [18]. These hollow structure devices had cross-sectional shapes that allowed for a natural flow of fluids inside the closed structure. The trapezoidal or hexagonal cross-sections of their cavities were fabricated by micromachining two silicon wafers with KOH etching and fusion bonding of etched wafers, respectively. Its fundamental principle is analogous to that of vibrating tube densitometers [19, 20], but SMR uses a small structure with the channel length of few hundreds of microns and channel height with the similar order of magnitude to the analytes such as

cells to sensitively measure suspended cells or biomolecules attached to a channel surface wall. The responsivity of the sensor increases when the size of the analytes and the channel height is designed as similar as possible. But to prevent the channel clogging, the height and width of the channel is designed more than 3 times larger compared to the size of synthetic particle samples. Accordingly, channel resonators of various sizes have been proposed to measure targets in various sizes as shown in Fig. 1.

In the first SMR, a sensor with a height of 3 μm and a width of 8 μm was proposed in consideration of the ease of fabrication by deposition of polysilicon sacrificial layer and silicon nitride as a structural material [14]. The resulting flat channels were easily integrated with electrical lines, allowing for further augmentation of the measurement methodology such as electrostatic actuation or piezoresistive sensing of the cantilever's vibration. Microfluidic channels enclosed inside a cantilever resonator are connected to external reservoirs to operate a flow of analytes. To enhance the measurement sensitivity, following works with vacuum packaging of SMR on the wafer scale supplemented such an approach by reducing the viscous air damping around the cantilever using glass frit bonding [21]. Compared to the resonators without channel operated in water before the SMR invention, the mass sensitivity was significantly increased to measure tiny biomolecules or single celled organisms such as bacteria. For example, the specific binding between biomolecules such as avidin and biotinylated bovine serum albumin was monitored in real-time. In addition, even different kinds of analytes can be continuously delivered to the sensor with pneumatic controllers through pressurized vials. Thus, the introduction of the devices with much easier operation and higher sensitivity extended the scope of application towards biomolecular detection.

Thereafter, the development direction of the SMR device was divided into two categories until today: expansion of the channel size for measuring large analytes, and reduction of the channel size for measuring small analytes. In the larger scales ranging from single to double digits microns, silicon MEMS-based channel resonators were mainly used to analyze the characteristics of cancer or tumor cells for disease diagnosis [14, 22–24]. For example, SMR with a sensor size of 8 μm at both channel height and width is proposed for measuring yeast cells. Afterwards, SMR with a 15 μm of height and 20 μm of the width is proposed for measuring mammalian cells. On the other hand, a channel size of couple hundred nanometers is required to measure even smaller objects such as a single virus with the size around 100 nm [25–27]. Thus, channel with a 700 nm of height and 2 μm of the width is proposed with the name of suspended nanochannel resonator (SNR) [28, 29].

Unlike the conventional MEMS approach with photolithographic process, nano-fluidic channels fabrication methods

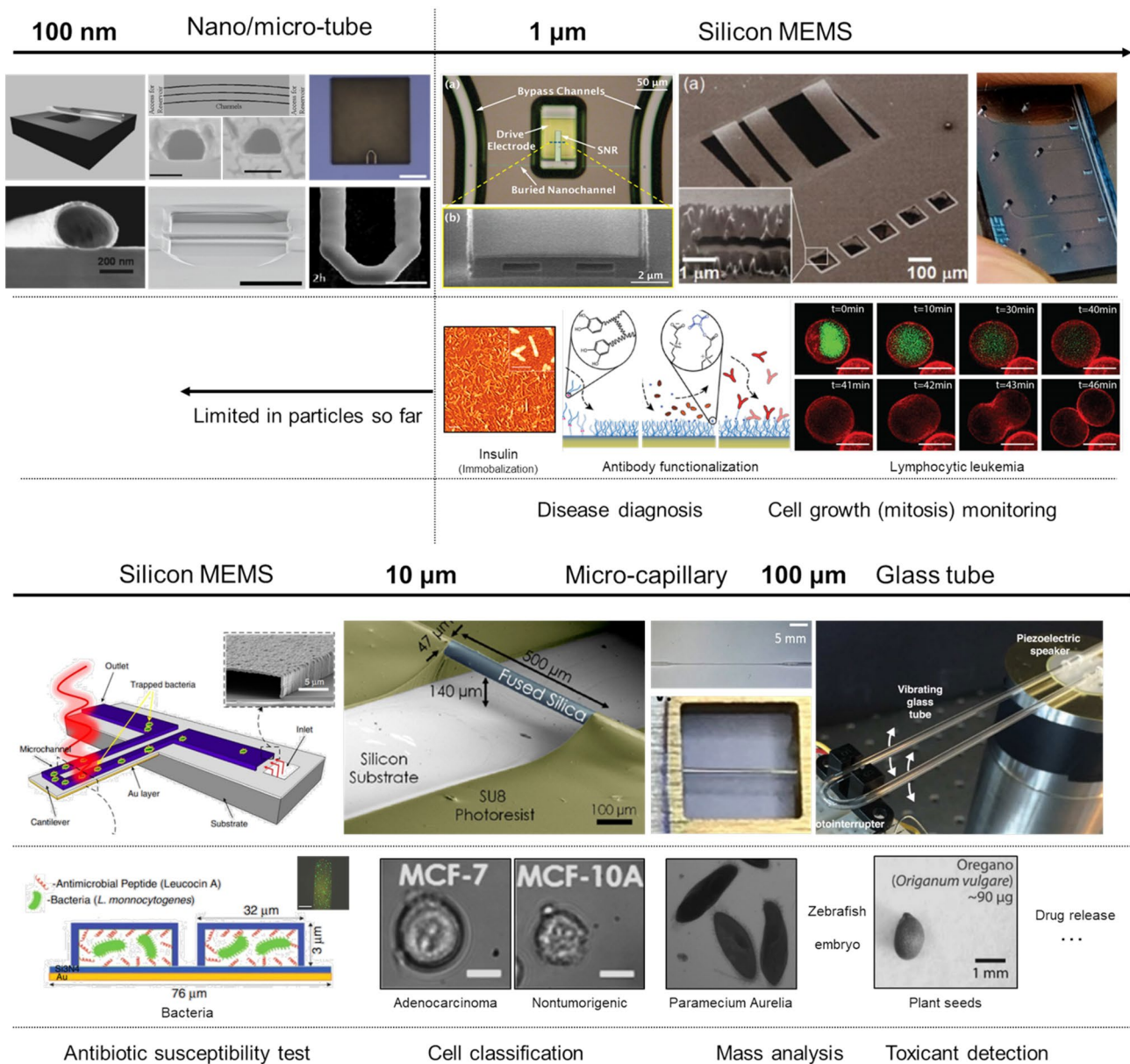


Fig. 1 Types of suspended channel resonators for bio-sensing application: While nano/micro-tubes under 100 nm were fabricated using unconventional methods, microchannels between 1 μm and 10 μm were fabricated by conventional silicon MEMS technology, and micro-capillaries or glass tubes over the 10 μm were fabricated by modifying the original tubular structure. Since their first introduction, applications with channel resonators over 1 μm have been expanded to many biological applications such as disease detection or cell classification. However, visible achievements with nanoscale channel resonators are still limited to characterization or measuring

synthetic measurables. Copyrights in nano/micro-tube: reprinted with permission from 2005 AIP Publishing [25], 2010 [26] and 2016 [27] American Chemical Society. Copyrights in Silicon MEMS: reprinted with permission from 2010 American Chemical Society [29], 2003 AIP Publishing [14], 2015 [51] and 2010 [22] American Chemical Society, 2019 Research Outreach [23] and 2016 Springer Nature [24] under CC BY 4.0. Copyrights in Micro-capillary and Glass tube: reprinted with permission from [33] and [34], both from 2019 American Chemical Society, 2017 Public Library of Science [32] under CC BY 4.0 (<https://creativecommons.org/licenses/by/4.0/>)

in tiny tubular cross sections were also proposed [25, 30, 31]. Compared to flat channels made by a photolithographic process, tubular channels reduce the dead volumes and create a more in vivo-like environment. Such structures are more favorable for cellular, molecular studies with fluid flow. One approach to fabricate such device is thermal removal

of sacrificial polymer nanofibers, deposited by electrospinning and encapsulated by a spin-on glass [25]. Following the deposition and depolymerization of nanofibers, they are encapsulated by a silicon dioxide layer and photoresist was spun on the silicon dioxide. Then, the silicon dioxide layer is dry-etched down to the substrate, and the remaining

photoresist is removed in oxygen plasma. Finally, the chip is heated to diffuse out the by-products, resulting in an elliptical channel. Silicon self-assembly [30] is another approach which utilizes surface energy minimization during high-temperature annealing [31]. After fabricating deep trenches or deep pillar-shaped holes on silicon substrate, annealing forces the silicon atoms to migrate near the surface. The shapes of resulting hollow space inside the wafer called a cavity are determined by the aspect ratio and their spacing of initial holes. Then, thermal oxidation and following selective etching forms the resonator structure along the self-assembled cavity. The fabricated resonators with the self-assembly process showed the feasibility of attogram-scale mass sensing [27]. So far, however, devices with tubular structures under 1 μm fabricated by unconventional methods have only measured calibration particle or physical properties of fluid, without specific applications in the biological field. It may be due to the fact that technological difficulties to monitor the thin and high frequency devices with large signal-to-noise ratio. Since its working principle is not fundamentally limited, advances in measurement technique may enable the operation of those devices in biological fields.

For larger measurement targets in the range of tens of micrometer to millimeters, some recent studies tackled a different limitation of the lithographic approach, resolving the expensive cost and low throughput incorporated with the device fabrication process. Instead of complicated MEMS fabrication, glass capillary/tubes have been introduced for the SMR devices [32]. These devices are advantageous in easy fabrication process by using its original tubular structure without geometry modification. More advanced approach in repeatedly producing these devices have been proposed, incorporating commercial hollow capillary with MEMS fabrication [33]. Such devices were also further customized, reducing the sensing part capillary size through thermal processing while retaining the size of the inlet and outlet [34]. The inexpensive and microfabrication-free

approach is advantageous by easily making over tens of micron-size channels for measuring relatively large analytes such as embryos [32], unicellular organisms [34] or plant seeds [32].

3.1 Basic operations

3.1.1 Principles

Mechanical resonance can be explained as the maximum vibration amplitude when the system's natural frequency (resonance frequency, f_R) is matched with the actuation frequency. The resonance frequency is represented with the spring constant (k) and the mass (m) of the system as shown in Eq. (1).

$$f_R = \frac{1}{2\pi} \sqrt{\frac{k}{m}} \quad (1)$$

When the small analytes such as synthetic particles, biomolecules, or cells are introduced to the resonator with effective mass (m_{eff}), the change in mass (Δm) causes a change in the resonance frequency (Δf_R) as shown in Eq. (2).

$$\frac{\Delta f_R}{f_R} = \frac{1}{\sqrt{1 + \frac{\Delta m}{m_{eff}}}} - 1 \approx -\frac{1}{2} \frac{\Delta m}{m_{eff}} \quad (2)$$

That is, the basic concept of measurement with SMR is to characterize how much the mass of the system has changed by tracking the resonance frequency. The relationship between mass and frequency shift can be first calculated by performing a calibration process using a reference mass using synthetic nanoparticles, and then measuring the frequency shift for analytes with unknown mass. The process including mass calibration with frequency shift and the new measurement is shown in Fig. 2. In addition, buoyant mass ($\Delta m = (\rho_a - \rho_f) \cdot V_a$) of the floating analytes with density (ρ_a)

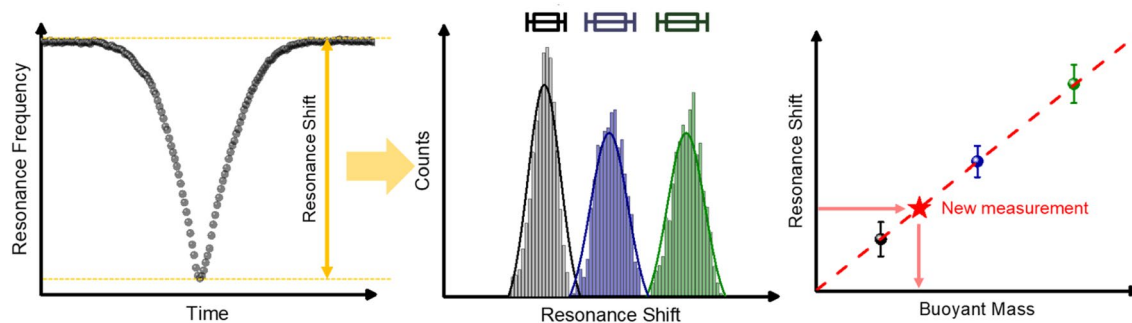
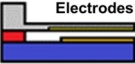

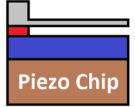
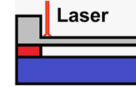
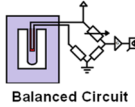
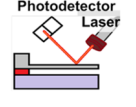


Fig. 2 A schematic illustration for representative buoyant mass measurement process including resonance data acquisition and mass calibration: The mass change of the SMR due to the analyte appears as a resonance shift, and the magnitude of resonance shift is accumu-

lated to be statistically analyzed. After performing calibration using synthetic particles with well-known buoyant mass, target analytes are injected into the SMR and their buoyant mass can be known by resonance shift measurements

Table 1 Schematic illustrations representing the methodologies of actuation and detection of suspended microchannel resonators (SMR) with their characteristics

	Actuation & Detection		Actuation		Detection	
	Capacitive (On-chip)	Piezoelectric (On-chip)	Piezoelectric (Off-chip)	Photothermal (Off-chip)	Piezoresistive (On-chip)	Optical (Off-chip)
Schematics						
Characteristics	Compact packaging	Individual actuation	Easy operation No additional fabrication	High frequency availability	Compact packaging	No additional fabrication
	Strong nonlinearity	Fabrication difficulties	High frequency limitation	Bulky setups Not suitable to bio-applications	Thermal noise limitation	Complex alignment

can be expressed to extract the density or the size information, by subtracting the fluid density (ρ_f) and multiplying its volume (V_a).

3.1.2 Actuation

There are three main types of actuation mechanisms used for SMR devices: capacitive, piezoelectric, and photothermal actuation as shown in Table 1. The methods of mounting the actuator on the channel resonator can be explained by two types. One is an on-chip method, where the actuator is placed inside a packaged chip during the fabrication process. The other is an off-chip method, in which an actuation voltage is applied outside from the packaged sensor. The on-chip actuation method requires more complex processes during the fabrication, but enables a compact packaging than the off-chip method. The capacitive (electrostatic) actuation is a representative of on-chip methods. It is operated by applying electric field between two electrode pads of coated metal on one side of the sensor and the confronting side of the cantilever substrate. In consideration of the pull-in effect, the distance between the channel resonator and the substrate is generally designed to have a sufficient gap. This method has the advantage of easy fabrication process compared to other sensor integration methods. However, it has strong nonlinearity as a natural characteristic of capacitive actuation. That is, the device cannot be operated in the full dynamic range [35]. The photothermal actuation is one of typical off-chip methods. Resonators are locally heated with the laser source that induces vibration from repetitive expansion and contraction of the cantilever material by photothermal energy conversion. Here, the laser is intensity-modulated with the same frequency of the resonator. However, the downside of photothermal actuation is the bulky setup and the need for precise alignment. More importantly, it is not suitable for

most bio-applications where constant temperature control is vital. The piezoelectric method which uses the piezoelectricity of converting electric charge into mechanical stress can be utilized as both on-chip and off-chip. In the on-chip piezoelectric method, electrical energy is directly applied to piezoelectric materials deposited on the channel resonator. In the off-chip piezoelectric method, the piezoelectric chip is tightly fitted to the channel resonator to transmit acoustic vibration through the structure. Off-chip actuation does not require an additional fabrication process, but it entails several disadvantages compared to the on-chip actuation. For example, if several sensors are simultaneously operated using an off-chip combined piezoelectric actuator, a voltage is applied to one piezoelectric chip by adding all signals to be applied to each sensor with a voltage adder [36]. In this case, when the several sensors have similar resonance frequencies, the adjacent applied signals may act like noise. In this aspect, on-chip actuation is more efficient when trying to drive multiple sensors at the same time because only the signal corresponding to each sensor is applied to the actuator. In addition, the acoustic vibration generated by the displacement of the piezoelectric material indirectly delivers the mechanical vibration to the resonator, thus less efficient in terms of high-frequency driving compared to other direct actuation methods. Here, the high-frequency driving is required when using a sensor with a high resonance frequency to improve the mass measurement resolution of small biomolecules.

3.1.3 Detection

There are four main types of detection mechanisms used for SMR devices: optical, piezoresistive, piezoelectric, and capacitive detection. Optical detection has been most widely used to measure the vibration of SMRs since they

require the optical system outside the devices (off-chip detection), without any need of a separate sensor integration process on the resonators. However, the optical systems require precise alignment for an accurate measurement and a bulky setup. In addition, thermal noise from the focused laser can affect the sensor's performance depending on the sensor material [14]. When measuring multiple sensors, the setup was configured to scan the laser or to allow the entire sensor to enter one beam spot, but this method has a limitation in the total number of sensors that can be measured at once. Piezoresistive sensing is the most used method for an on-chip detection [37]. A piezoresistive material is deposited on the cantilever and the resistance change due to deflection is monitored with a balanced bridge circuit. This method is advantageous with easy fabrication and compact packaging as well as no limitation of the number of sensors. However, the thermal noise from the heat dissipation of piezoresistive material can limit the detection capability. Piezoresistive detectors are recommended to be used with piezoelectric actuation because electrostatic actuators may affect the accuracy of piezoresistive sensing due to electrical couplings. An on-chip piezoelectric actuator [38, 39] is also used as the sensor, which measures the voltage generation from cantilever deflection in the piezoelectric material. Piezoelectric material is less affected by thermal noise compared to piezoresistive or optical detection methods and shows good linearity. However, the doped material can act as an added mass and degrade the sensitivity. Capacitive sensing uses the same principle with the capacitive actuation, measuring the voltage generated by the change in distance between electrodes [40]. The fabrication process of capacitive-sensing devices with integrated electrodes is relatively easier compared to that of devices with piezoelectric or piezoresistive electrodes for its material selectivity. However, nonlinearity of the sensor is a limitation again in detection.

3.2 Advanced operations

3.2.1 Trapping for single cell growth measurements

SMR, which has the advantage of measuring single cells individually, could easily determine either the positive or negative growth rate by continuous monitoring. First method to continuously monitor a single cell is by static trapping, as shown in Fig. 3a. Static trapping uses a mechanical structure to physically trap the cell near the tip of the resonator. In doing so, a structure similar to the cell size is integrated inside the channel in the form of columns, docks, and so on. Cell capture is detected as a stepwise change in the resonant frequency due to the change in mass inside the cantilever. In addition

to buoyant mass of cells, dry mass could be measured using heavy water or DI water as the flow medium [41]. However, mechanical trapping bears several drawbacks [42]. First, when the trapping structure is placed far away from the cantilever apex, such imperfection introduces an undesired disparity between the true resonance frequency (cell located at the apex) and the measured resonance frequency. Second, the shear stress caused when the cells are escaping the confined structure lowers the viability of cells [43]. Similarly, unwanted surface roughness resulting from the additional fabrication process could harm the cell's condition.

To resolve these limitations, trapping methodologies without contact or friction between the cells and resonator structures were proposed as shown in Fig. 3b. One method utilizes the centrifugal force resulting from the strong vibration of the cantilever [29, 37]. Here, the cantilever behaves as an acceleration system to trap the analytes at the end of the cantilever. As a result, cells do not experience a large degree of strain due to the non-contact operation, along with the confirmation of the cell's exact position at the tip of the resonator. However, in lieu of this advantage, the technique loses selectivity in terms of the number of analytes. When one cell is already trapped inside the resonator, other analytes can be continuously accumulated. In addition, measurement error occurs from the frequency drift when we want to analyze the time dependent change of the analyte.

Thus, dynamic trapping technique [44] was proposed as shown in Fig. 3c to circumvent the above-mentioned limitations where the single particles move back and forth inside the cantilever repetitively by alternating the flow. The mass of the particle is measured twice for each repetition, reversing the flow when the cell transiting the apex of the resonator is detected. The dynamic trapping technique is robust against environmental drifts which static or inertial trapping approaches are prone to. Specifically, fast and repeated measurement of dynamic trapping minimizes the effects of resonance drift due to environmental errors such as changes in ambient temperature. The refinement allowed for novel discoveries including the size dependence of cell growth rate and the need of active growth and division balancing for bacterial, yeast, and mammalian cells. However, compared to static trapping or inertial trapping where stepwise change occurs, the software filtering window in dynamic trapping is narrow. Thus, if the measurement target passes through the resonator quickly, the post-processed signal may underestimate the real change in resonance. For this reason, if there is no drift during the measurement, static trapping or inertial trapping methods have better measurement resolution than dynamic trapping.

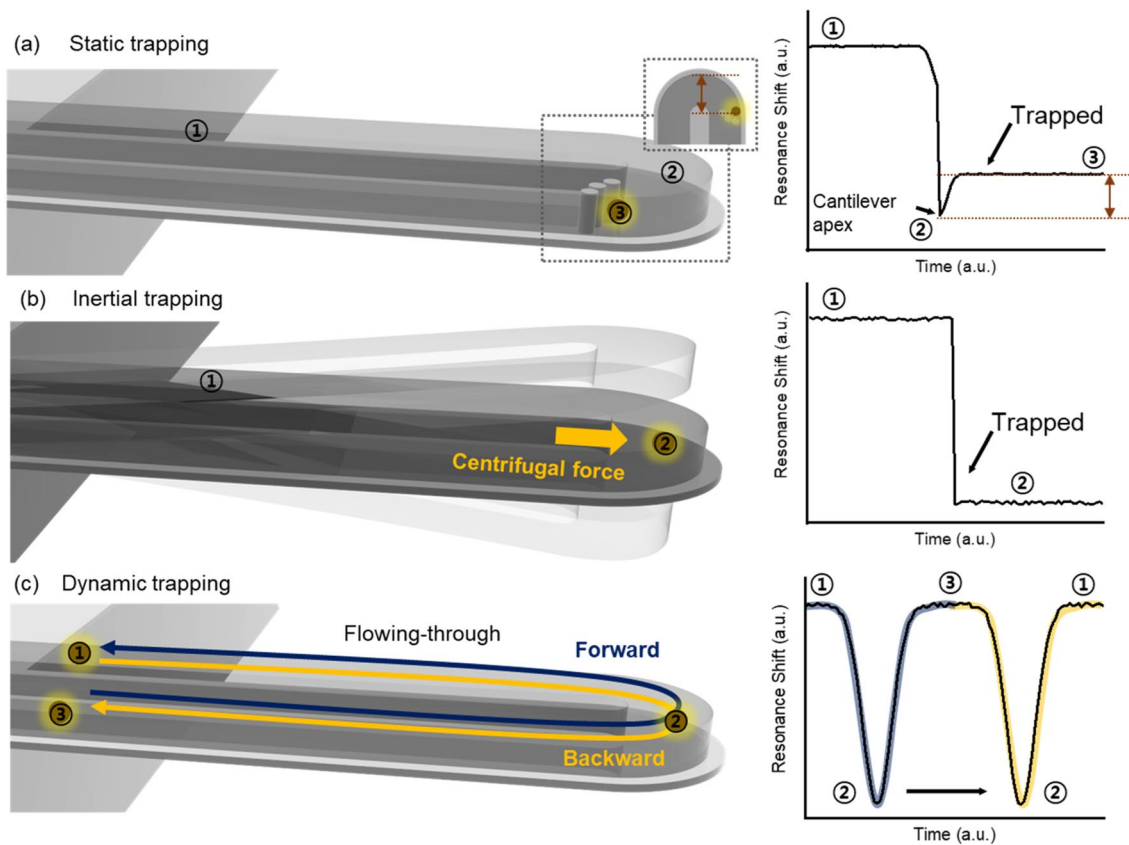


Fig. 3 Schematic illustrations and pseudo data of resonance shift in time showing various trapping methods for single cell growth measurement: **(a)** Static trapping uses mechanical structures. Resonance change is maximized when the analytes are passing through the cantilever apex, and maintained when it is caught by the mechanical trap. As the structure is far away from the end of the cantilever, the real change of the resonance may be different from the maximum change of the resonant frequency. **(b)** Inertial trapping uses centrifugal force during vibration. This method requires strong actuation of the resona-

tor when individual analytes are passing through the cantilever apex. Individual trapping occurs depending on the comparative difference between centrifugal force and drag force of each analyte, which can possibly cause a stepwise change in the resonant frequency of analytes passing through the resonator. **(c)** Dynamic trapping uses automatic pressure control by changing the flowing direction of the analytes. Each number represents the position of the analytes and the corresponding resonance shift

3.2.2 High-throughput measurements

Trapping techniques to measure growth rate of cells are limited to a low throughput: single cell per one resonator. However, biological industries focusing in drug development or disease diagnosis demand for a higher measurement throughput. In that sense, diverse approaches have been made in tackling such challenge as shown in Fig. 4. The first effort was serial SMR arrays [45] with the concept of embedding delay channels between the resonators to provide time intervals between resonators for cell growth as shown in Fig. 4a. 50 mm delay channels result in a transition time of about 30 s between individual SMR at a typical SMR flow rate. The actual SMR devices measuring the growth rate are few hundred micrometers long. For resonance measurement, lasers cover all the cantilevers and the corresponding signals detected by a photodetector are fed back to multiple phase

locked loops (PLLs). The number of PLLs is same as that of cantilevers. Then, the piezo-ceramic actuator is operated in reference to the added signals from the multiple PLLs, controlling each cantilever with its resonance frequency. The technique also incorporates bypass channels by randomly selecting and floating analytes into the cantilever array channel to utilize various sample delivery and measurement. This technique increased the throughput of mammalian cells or bacteria over 60 targets per hour. Subsequently, active loading technique into a bypass channel [46] was added to further increase the measurement throughput up to 386 analytes per hour, shown in Fig. 4b. This approach triggers active pressure control when analytes flow near the passage by optical monitoring at the inlet of the channel.

For a population study instead of a single cell analysis, the bypass channels were parallelized to incorporate the previously introduced high-throughput aspect,

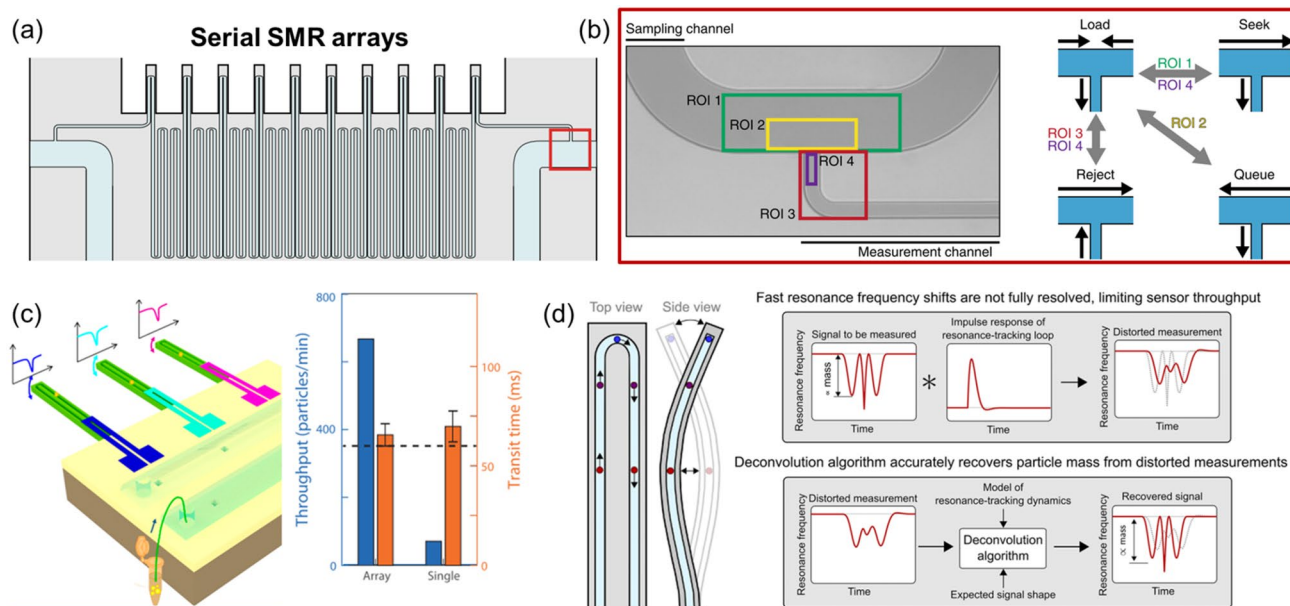


Fig. 4 Various efforts in fabrication and operation methods for high throughput measurement: **(a)** Serial SMR arrays for growth and mass accumulation rate measurement of a single cell. Delay channels between the SMR arrays give a specific time interval to the measurement. **(b)** Active loading operation method in serial SMR arrays with a pneumatic control which is triggered by optical monitoring. By reducing the time interval of analytes injected from the bypass channel to the SMR sensing area, it has higher throughput compared to passive loading. Reprinted with permission from [46], 2018 Springer Nature under CC BY 4.0 (<https://creativecommons.org/licenses/by/4.0/>).

shown in Fig. 4c. However, since optical detection method limits the number of measurable sensors, a different resonance measurement methodology was required for such approach. Namely, piezoresistive sensing [37] was implemented for each cantilever [28]. The signals obtained from piezoresistive sensors were added to the piezo-ceramic actuator through each PLL as described in Fig. 4a. The parallel SMR with piezoresistive sensing approach increased the throughput up to 40,000 particles per hour.

As the measurement interval between particles became narrower, the possibility of more than one samples flowing into one cantilever inevitably increased. The anomaly leads to measurement errors with doublet occurrences. While manually controlling the concentration could prevent doublet occurrences, it also limits the throughput. Therefore, a data post-processing approach by deconvolution of the signal was proposed [47], operated on the same sensors as shown in Fig. 4d. In this way, the throughput was improved by 24,000 particles per a minute while maintaining a variation 4 times smaller than the Coulter counter, a commercial equipment for counting the cell size.

by/4.0/). **(c)** Parallel SMR arrays for individual cell measurement without the delay channels, integrated of piezoresistive sensor for simultaneous and separated detection. The introduction of the parallel channel is to measure the population faster, rather than looking at the growth rate of the cells like the purpose of the delay channel. Reprinted with permission from [28], 2020 American Chemical Society. **(d)** Deconvolution method for analyzing flowing analytes faster than measurement bandwidth. Reprinted with permission from [47], 2019 AIP Publishing

3.2.3 External temperature control

Temperature control realizes three objectives: (1) decreasing the measurement errors of resonance frequency from temperature drift or fluctuation, (2) maintaining appropriate physiological conditions for biological samples, and (3) modulating temperature for specific application such as phase transition monitoring of biomolecules. First objective is due to the fact that the properties which affect the resonant frequency are also prone to temperature change. To minimize the long-term drift in resonance frequencies of the SMR (approximately 100 mHz over 10 min in the reference [48]), constant temperature control is required to both the water circulator mounting clamp and the sample holder in pressurized vials. In addition, maintaining an ideal temperature is crucial for optimal cell growth. Specifically, temperature control near 37 °C is mainly used in SMR measurements where most mammalian cells thrive. The temperature is maintained using surface-mounted thermometer connected directly onto the device and thermoelectric controller [44]. Other special applications such as phase transition studies also require temperature control. In the reference [49], DNA melting is characterized by monitoring DNA's thermal

duration with the temperature of SMR in real time during the melting state of DNA. For doing so, SMR is operated with an external temperature controller, which consists of resistive heater and a thermocouple on the cantilever base. For both melting and premelting states, SMR provided a framework to calculate the specific heat capacity and storage and loss factors of the overall system, and established a platform for quantifying the thermo-mechanical behavior of DNA.

4 Biomedical applications

The detection method using SMR can be divided into two approaches: 1. buoyant mass measurement by resonance frequency shift and 2. multi-modal measurement with integration of other detection techniques, as shown in Fig. 5. The measurement methodology of buoyant mass is divided into flow-through mode and surface binding mode, depending on whether the analytes are measured when they are passing with the flow or adsorbed inside the channel. Multi-modal measurements are also divided into two types depending on whether the measurement of additional parameters is performed simultaneously along with the mass measurement (*in-situ*) or either before/after the mass measurement (*ex-situ*). For *in-situ* measurements solely relying on the SMR, the intrinsically transparent window of SMR is used, or structural modification with new design and fabrication is added to the general SMR device. For *ex-situ* measurements requiring instruments other than the SMR, measured samples should be collected and used for additional measurements. While *in-situ* measurements offer both individual (or single cell) and group (or population) studies, *ex-situ* measurements offer group study only to date.

4.1 Buoyant mass measurements

4.1.1 Flow-through mode

As discussed in previous sections, the basic operation of SMR measures buoyant mass as the fluid containing analytes continuously flows into the suspended microchannel. Flowing-through measurement is a method of measuring the difference in mass while fluid is introduced into a channel when the analytes are suspended in the fluid. Initially, a histogram of the mass is obtained with the hundreds of analytes such as synthetic particles or bacteria. Then, single cells are measured repeatedly with an iterative passage to continuously observe the mass change. SMR could also calculate the actual mass or density by measuring the ratio of cell mass to volume, representing a weighted mean of all cellular components' densities [41]. In doing so, after escaping from the cantilever of the fluid by switching the bypass channels with different fluids, a cell is retracted back to the SMR with a different density. Fig. 6a demonstrates the decrease in volume when using this technique, where the first 24 h shows the most dramatic change in cell volume for the entire measurement periods. Subsequently, serial SMRs were developed to improve the measurement throughput as discussed in the previous section. Namely, by grouping frequency peaks from the same cell, the mass accumulation rate (MAR) was analyzed from the change in buoyant mass over time. Addition of particles with invariant mass such as polystyrene as a calibration sample allowed for more obvious distinction of cell characteristics. The serial-SMRs also discriminated the various types of single gram-positive and gram-negative bacteria and observed the effects of antibiotics during the growth of bacteria [45].

Following the measurement of growth rate was *in-situ* monitoring of MAR during a drug injection process. As shown in Fig. 6b, such tandem measurements enabled a prediction of therapeutic response based on a single cell level measurement. In the reference [46], a sample of tumor cells were separated from the patient to be diagnosed, and

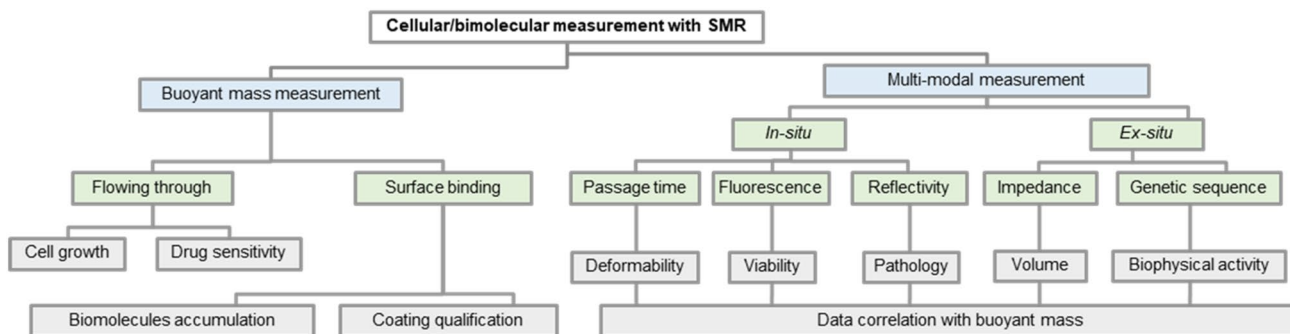


Fig. 5 Summary chart of the methodology for cellular/biomolecular measurements with SMR

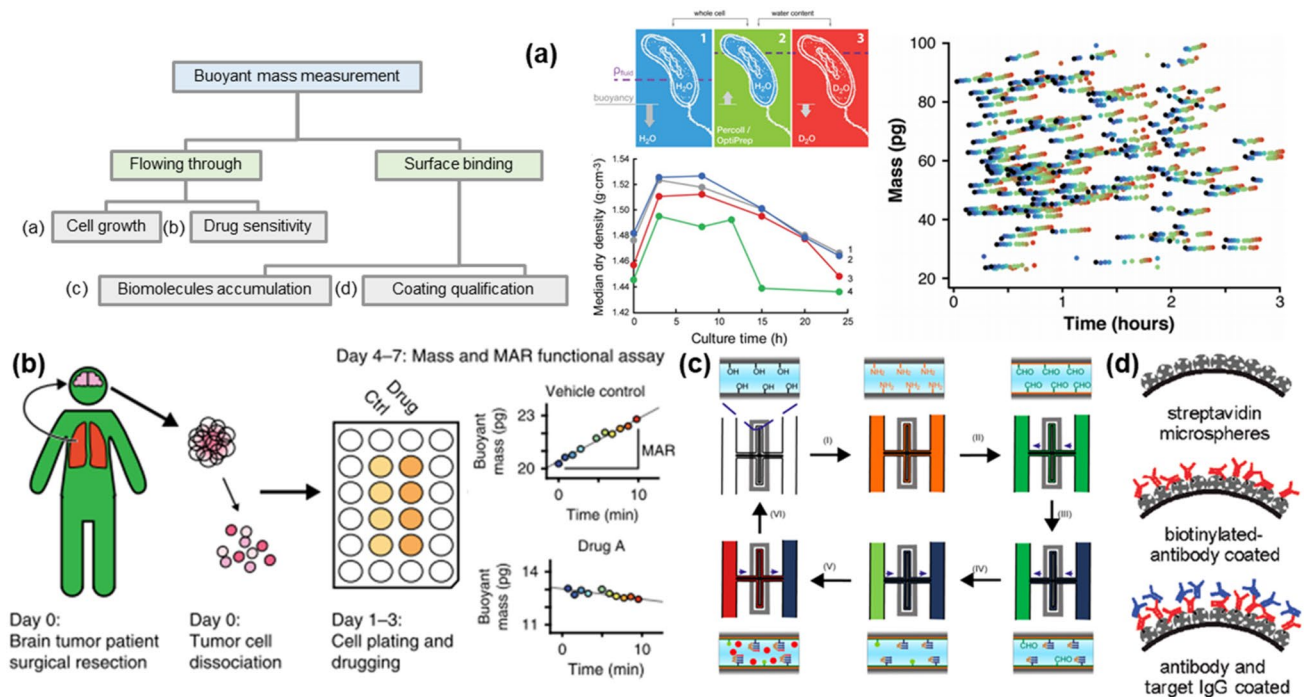


Fig. 6 Buoyant mass measurements: **(a)** Schematic illustration of cell growth monitoring in real time with the single (left) and the serial (right) SMRs. In single SMR, drug density can be calculated by exchanging medium and measuring buoyant mass twice. In serial SMRs with delay channels, multiple targets are simultaneously measured in real-time. Reprinted with permission from [41], 2013 Public Library of Science under CC BY 4.0. **(b)** Schematic illustrations of workflow to predict therapeutic response with drug injection. From the patient, tumor cell is collected and its mass accumulation rate is comparatively analyzed using control samples and drug-injected

samples. Reprinted with permission from [46], 2018 Springer Nature under CC BY 4.0 (<https://creativecommons.org/licenses/by/4.0/>). **(c)** Schematic illustration of SMR utilized in biomolecular detection by surface binding of mass measurement. Reprinted with permission from [51], 2015 American Chemical Society. **d** Schematic illustrations of streptavidin-functionalized microspheres for sensitive measurement of coatings with targeted antibody-antigen binding. Reprinted with permission from [52], 2012 American Chemical Society

waited long enough for a response to the drug for at least one day. The drug was maintained in the same environment with the untreated control sample during the wait. Next, the efficacy of a drug was determined by measuring and comparing the buoyant masses for both the control samples and drug-treated samples. This entire process well-matches with the ideal characterization of therapeutic susceptibility, which shows small sample loss, a subpopulation analysis, and strong measurability of single or combination of drugs. The most popular application with the similar approaches is the drug sensitivity measurement especially for the cancer treatment. Although a number of researches have been studied on the treatment of cancer in modern medicine, it is still not well understood how an individual patient will respond to the specific therapy. If cancer cells collected from the patient can be used to predict each drug responsiveness, it is expected to maximize treatment efficiency and patient survival rate. In the reference [17], two cancer cell types known to be viable and proliferate in suspended cell culture were used: glioblastoma (GBM) and acute leukemia. By measuring the MAR of cells with or without specific

cancer therapeutics and comparing those two groups, it is possible to predict how much effective the therapy would be for the patient.

4.1.2 Surface binding mode

Based on resonance measurements for detecting the mass change, SMRs can identify not only suspended cells in liquid but also the biomolecules (Fig. 6c). To realize high sensitivity and specificity, surface functionalization with appropriate chemical coatings are used [50]. In detail, chemicals are treated to the inner walls of SMRs to capture the analytes in a stationary accumulated manner unlike measurement of buoyant mass where cells are streamed along the fluid. The mass of the accumulated subject is *in-situ* measured by tracking the resonance during the biomolecule injection. There are three conventional methods of surface functionalization. The first is specific binding known as immobilization, which uses antigen and antibody integration to catch the biomolecules. For example in [51], Insulin seed fibrils were first covalently immobilized on

the surface by injecting buffer, followed by the introduction of seed fibril solution to the aldehyde groups. Then, the growth of insulin seed fibrils is measured during its exposure to monomer solution. The exact mass added during the process can be quantified by the difference in resonance frequency before and after the injection of each layer. In addition, as reported in the reference [22], the resonant frequency was measured when a cancer biomarker, activated leukocyte cell adhesion molecule (ALCAM), was introduced into the channel after functionalizing the SMR inner wall. Concentrations were quantified within a physiologically relevant range (10–1000 ng/mL) using a differential measurement scheme.

The second is affinity binding, which use biotin as an affinity tag and antibody to catch the biomolecules. In the reference [50], binding was observed in real time with injection of goat anti-mouse IgG into the functionalized resonator with poly(ethylene glycol)-biotin and neutravidin by monitoring the resonance frequency. Before adsorption of bindings or after the measurement of biomolecules, the surface can be easily cleaned and regenerated with a piranha solution. The last is hybridization between nucleic acid, which is commonly used in RNA or virus detection. However, this method is yet to be applied as an SMR technique for measuring biophysical properties.

Compared to previous label-free measurements with micromechanical structures, this channel resonator enables quick exchange of fluid samples and analytes, as well as the analysis of precious samples with a minimum consumption. Furthermore, as shown in Fig. 6d [52], a conventional approach of streaming the measurement subjects was also developed to detect coatings of chemical materials. The fluid density was matched with the density of the particle core for measuring buoyant mass of the coatings. Such modification allowed for an individual quantification of surface functionalized micro-particles, detecting differences in coating thickness or number of coated layers of proteins.

4.2 Multi-modal measurements

While previous SMR platforms allowed for high-throughput cell mass and MAR measurement, they were limited by incompatibility for further meticulous investigations since the mass alone is not sufficient to classify two different cells that have very similar cellular masses. Thus, few approaches integrating the multi-modal analysis with the previous mass measurement have been introduced to identify cellular groups and to correlate other physical properties along with the buoyant mass. The integration of several technologies will show higher identification by comprehensively considering the various characteristics of the analyte.

4.2.1 *In-situ* stiffness measurements

When the cells are subject to a variety of confined geometries, shear stress within the individual cells significantly affects each density or the volume, depending on the biophysical properties of each cell. Specifically, high metastatic cells are more deformable than weak metastatic cells, as demonstrated in various studies that have attempted to investigate the mechanical properties of cancer cells. Thus, to distinguish the normal and cancer cells, a wide range of approaches for measuring the various properties of single cells have been developed to investigate such phenomenon with engineering tools. Single cell approaches to measure deformability were firstly studied with the open-end hollow structures [53, 54] such as micropipette aspiration or channel cantilever with a nozzle. As for the micropipette aspiration [55], a large orifice is used with applying negative pressure for suction of the deformed cells. The stiffness is characterized by the diameter of pipette orifice, applied pressure, or suction velocity, etc. However, these technologies have crucial limitation in low throughput and *in-vitro* environment. Thus, a different approach of monitoring the behavior of a cell during the fluidic constriction was introduced, studying the viscoelastic properties of cells *in-vivo* as shown in Fig. 7a. In the reference [16], by adding a constriction channel (6 μm wide and 50 μm long) along the channel near the end of the cantilever (20 μm wide and 316 μm long), the passage time of a cell as it transits through the constriction is extracted. Single-cell buoyant mass measurements integrated with passage time information enable differentiating cell lines with similar buoyant mass but with different viscoelastic characteristics [56, 57]. In the reference [57], it was claimed that various biological activities that can appear in cells, such as protein synthesis inhibition, cell cycle arrest, protein kinase inhibition, and cytoskeletal disruption, lead to unexpected relationships between deformability, density, and volume. This suggests that multi-modal measurements of biophysical parameters detect more unique properties than measuring only a single parameter. Such characteristic is also applied in distinguishing cancer cells from normal cells. In the paper [58], it is shown that deformability and frictional properties are associated with one of the genetic alterations known to govern cancer cell metastasis. Deformability differences between circulating tumor cells and the normal blood cells [16] are also assessed by utilizing such finding. This method of measuring buoyant mass and deformability of a single cell helps elucidate the biophysical properties of cancer cells in the processes involved in circulation and metastasis without the help of specific biomarkers. However, the confined geometry must be different depending on the measurement sample size, an aspect to be considered before the fabrication process. In addition, such method bears limited viability since the

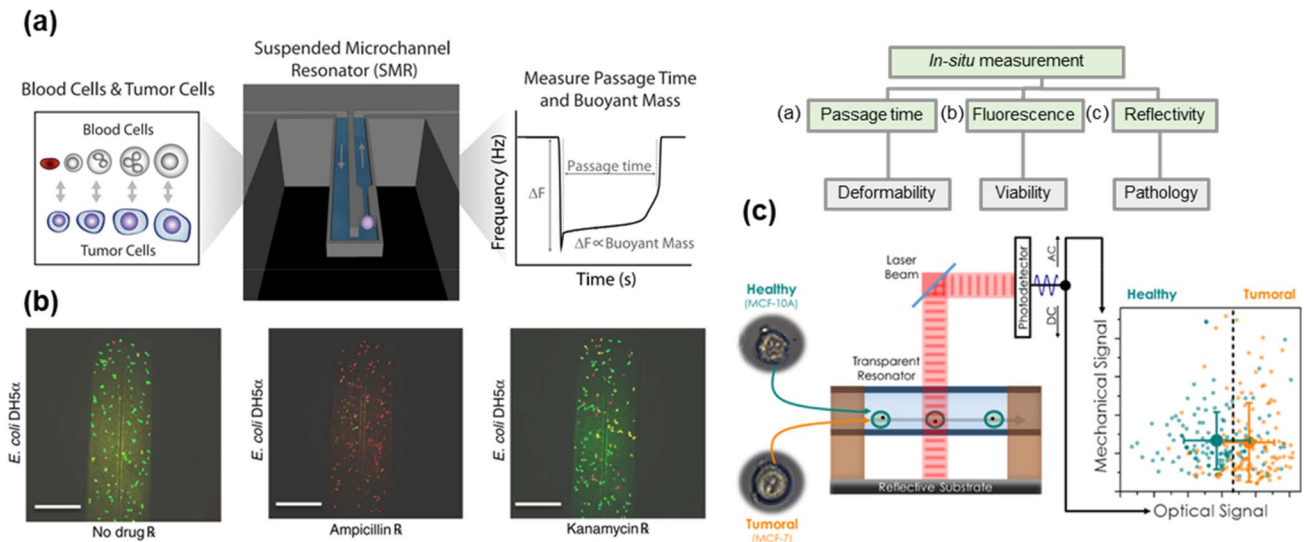


Fig. 7 *In-situ* multi-modal measurements: **a** Schematic illustrations showing cell passage time-based analysis when various cells are streamed into the confined structures. Reprinted with permission from [16], 2015 Springer Nature under CC BY 4.0 (<https://creativecommons.org/licenses/by/4.0/>). **b** Confocal microscopy images of the antibiotic–bacteria interaction after exposure to drugs where a fluorescence dye of live/dead viability kit was used to stain living

cells green and dead cells red. Reprinted with permission from [24], 2016 Springer Nature under CC BY 4.0 (<https://creativecommons.org/licenses/by/4.0/>). **c** Optical reflection analysis integrated with the buoyant mass measurement to increase cell pathology selectivity. Reprinted with permission from [33], 2019 American Chemical Society

sample undergoes continuous contact in a confined channel. To resolve these problems, a completely noninvasive method is proposed by analyzing the effect of acoustic waves on vibration of cells to measure their stiffness [59]. According to the theory of resonance, in the second vibration mode, no resonance frequency shift would be observed regardless of the added mass of analytes at the node where there is no vibration amplitude. Acoustic scattering was inspired from the fact that there is always non-zero deviation in the node and it varies depending on the stiffness of analytes, which is explained as an acoustic wave generated inside the channel while the cantilever vibrates. As a result, it was proved that the stiffness significantly changes during the mitosis while there is no change observed in the interphase of the cell.

4.2.2 *In-situ* optical property measurements

Similar to discovering additional physical parameters as discussed in previous sections, there are studies that have attempted monitoring and classifying cells with optical based measurements by mixing fluorescence dyes to the samples or by using the optical properties of analytes. Integration of fluorescence with SMR technology enables the result verification of cell classification from buoyant mass measurement [56] or linked property measurements by concurrent monitoring of cell size and mass over multiple generations in a cell cycle [60]. Fluorescence measurements were performed at the optical window in the bypass channel

after the SMR, near the channel entrance before entering the SMR, or on the collection plate placed on the downstream. For this analysis, the channel must be transparent to optically observe the sample. One application using such approach is single labeled proteins detection which measures the bursts in reflected laser's intensities while single cellulase molecules labeled with several Rhodamine-red fluorophores are diffused through the channel [61]. These bursts of reflection intensities over time incorporate the number of fluorophores per molecule. Another application is the cell viability measurement, where two different fluorescent dyes are stained on living and dead organisms as shown in Fig. 7b [24]. Specifically, by counting bacteria through the thin and transparent silicon nitride channel using fluorescence images, viability of bacteria in a specific environment is determined. This work discovered that most Escherichia coli (*E. coli*) exposed to ampicillin died (red staining), whereas 75% of the *E. coli* exposed to kanamycin remained active (green staining). Along with the optical classification, conventional buoyant mass measurement techniques such as resonance frequency and deflection measurement were also operated for maximal reliability of the above acquired results.

The combination of SMR with fluorescence has also been used to more accurately measure surface-bound mass. In the paper [62], the microchannel facing the side of the cantilever was functionalized with an anti-insulin antibody to measure the surface insulin by mass. In addition, by demonstrating the degradation of immobilized human recombinant by

various concentrations of proteinase K solution, the enzymatic reaction progress was monitored using the resonance frequency. Here, the surface functionalized process was optimized while monitoring with fluorescence.

In addition to fluorescence, reflectivity is used as another indicator for classifying cells [33, 63] as shown in Fig. 7c. In the paper [33], mechano-optical analysis is performed using a glass capillary. In detail, a laser is focused on the transparent capillary channel to extract the intensity from the optical reflectivity, while mechanical responses are simultaneously monitored. This approach enables the pathological discrimination between healthy and abnormal cells of the same tissue type. With this approach, MCF-7 human breast adenocarcinoma cells and MCF-10A non-tumorigenic cells are successfully classified with a throughput of 300 cells per minute.

4.2.3 *Ex-situ* volume measurements

Although SMR is conventionally used as a tool for individual cell measurement, a population study can also be conducted by collecting cells into groups before or after passing the sensor. In this case, a conventional cytometry is used for the reference as well as obtaining the biophysical measurement with SMR as shown in Fig. 8a [64]. Two different parameters were measured by combining SMR technology to measure mass and Coulter counting technology to measure volume. Afterwards, technology has been developed so that the mass and volume can be simultaneously measured inside a dual SMR by replacing the medium during the

measurement of the same particles [65]. Unlike the previous study in which volume measurement was measured as a group, it is possible to additionally extract information such as the density of individual cells since volume can be matched in a one-to-one correspondence with mass. The volume measured using this method was verified with a Coulter counter. When compared to a commercial Coulter counter, cell volume measurements from the SMR are proven to be nearly identical, which suggests that SMR measurement process does not affect to physical states of the cell.

4.2.4 *Ex-situ* genetic information measurements

There are also studies that have attempted linked measurements of individual cell's biophysical properties along with gene expression [66]. According to previous studies, the characteristics of the cell genome of a single cell can be measured using techniques such as RNA sequencing [67]. In this study, genetic analysis demonstrated the feasibility of resolving distinct transcriptional signatures associated with subtle differences in single cell mass and growth rates. As shown in Fig. 8b, an automated single-cell collection system is established at the outlet of the serial SMR. Specifically, the peak detection at the final SMR cantilever triggers a 3D motorized stage to place a PCR tube containing lysis buffer to capture each cell. Such a novel scheme allows for a high-throughput measurement of mass, growth rate, and gene expression. To validate the linkage of mass related measurements from SMR and the genomic post-analysis, this work presents characterization of CD8 + T cell activations, linkage

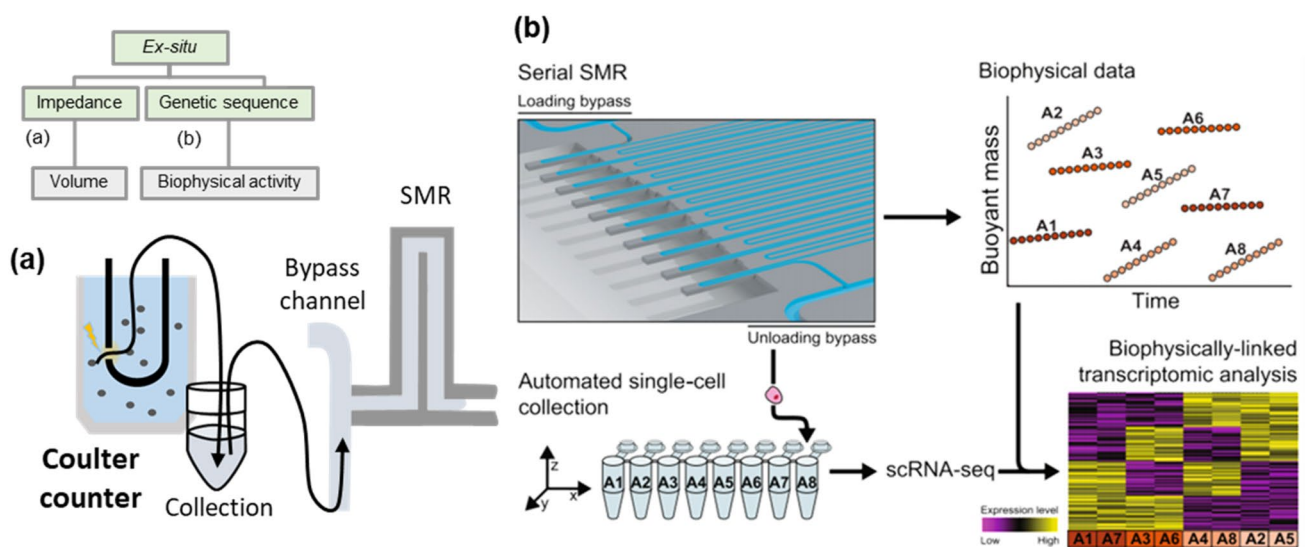


Fig. 8 *Ex-situ* multi-modal measurements: **a** A schematic illustration of showing Coulter counter for cell volume measurement integrated with SMR technology for buoyant mass measurement. Prior to injecting analytes to SMR, samples are collected after volume measurements. **b** A schematic illustration of a work flow with automated

single-cell collection after the array of SMRs, followed by single cell RNA sequencing correlated to the biophysical analysis. Reprinted with permission from [66], 2018 Springer Nature under CC BY 4.0 (<https://creativecommons.org/licenses/by/4.0/>)

between biophysical and gene expression measurements, and characterization of single-cell biophysical heterogeneity of patient-derived cancer cells. The augmented SMR platform has pioneered linked-measurements of single-cell biophysical properties and gene expression, providing a tool to solve unanswered questions such as DNA sequencing [68], epigenomic characterization, or multi-omic measurements of single cells [56].

5 Conclusion and Future Outlook

In this review, SMR technologies in a biomedical view have been discussed with development history, operation methodologies, and key applications. In terms of development, biomedical approaches with SMRs mostly relied on MEMS-fabricated structure for its technological maturity. Afterwards, commercially available structures such as hollow capillaries were also adapted to minimize efforts in the fabrication process. For operation methodologies, basic working principle and actuation/detection methods were discussed. Advanced approaches to trap the single cell inside the sensor and to increase the measurement throughput are followed. In cellular or biomolecular detection, we have organized the detection scheme in two groups as application based on buoyant-mass sensing and multi-modal measurement integrated with other detection methods. Although applications based on buoyant mass measurement such as growth rate, cell classification, or drug susceptibility testing could quickly and precisely discover new biological findings, measurement with a single parameter inevitably incorporates a fundamental limitation. Thus, various detection methods such as fluorescence microscopy, reflectance analysis, cell counting with Coulter principle or genetic analysis have been integrated into the channel resonator to further widen the applications after the initial invention of SMRs. So far, these approaches can be divided into *in-situ* analysis matched in serial with single cell mass measurement by SMR, and *ex-situ* group analysis for integration with other commercial measurement technologies. Here, if commercial measurement technology is modified and integrated within SMR, analysis methods that were previously only possible with group analysis can be used as individual target analysis, which enables single cell-based measurement to be further expanded. In the future, development of SMR technology will show a trend similar to that of atomic force microscopy (AFM) technology. Although AFM was first introduced for the purpose of obtaining the topography of nanoscale structures, it has been extended to various fields and biomedical applications, such as analyzing physical characteristics of cells or the hydrophilicity of the surface. Similarly, despite the limited number of research groups using SMR technology today, various developments are expected to be

introduced in the future. For example, there is a sufficient possibility that the system will be developed to the familiar shapes to bio-researchers such as pipettes not just with a channel resonator by MEMS fabrication. In addition to the platform development, other detection technologies will be integrated within or outside of SMRs with increasing interests in the chemical, thermal, electrical, or magnetic properties of biological matters and functional materials. Synergy between the conventional biomedical measurement methods and the more recent multi-modal measurements will introduce exciting opportunities to contribute towards the advancement of biological and biomedical studies.

Funding This research was supported by the National Research Foundation of Korea (NRF) grants funded by the Korean government (Ministry of Science and ICT) (NRF-2020R1A2C300488512 and NRF-2020R1A4A200272812).

Declarations

Conflict of interest The authors declare that they do not have any conflicts of interest.

Ethical approval This article does not contain any studies with human participants or animals performed by any of the authors.

Consent for publication All authors have consented to the submission of their work to the journal.

References

1. Lue N, Choi W, Popescu G, et al. Quantitative phase imaging of live cells using fast Fourier phase microscopy. *Appl Opt*. 2007;46:1836. <https://doi.org/10.1364/AO.46.001836>.
2. Joo C, Akkin T, Cense B, et al. Spectral-domain optical coherence phase microscopy for quantitative phase-contrast imaging. *Opt Lett*. 2005;30:2131. <https://doi.org/10.1364/ol.30.002131>.
3. Curl C, Harris T, Harris P, et al. Quantitative phase microscopy: a new tool for measurement of cell culture growth and confluency in situ. *Pflügers Arch*. 2004;448:462–8. <https://doi.org/10.1007/s00424-004-1248-7>.
4. Chalut K, Brown W, Terry N, Wax A. Quantitative phase microscopy with asynchronous digital holography system. *Opt InfoBase Conf Pap*. 2007;15:3047–52.
5. Gertler R, Rosenberg R, Fuehrer K, et al. Detection of circulating tumor cells in blood using an optimized density gradient centrifugation. In: Allgayer H, Heiss MM, Schildberg FW (eds) *Molecular Staging of Cancer*. Springer Berlin Heidelberg, Berlin, Heidelberg. 2003;162. https://doi.org/10.1007/978-3-642-59349-9_13.
6. Rosenberg R, Gertler R, Friederichs J, et al. Comparison of two density gradient centrifugation systems for the enrichment of disseminated tumor cells in blood. *Cytometry*. 2002;49:150–8. <https://doi.org/10.1002/cyto.10161>.
7. Mori K, Oura T, Noma H, Matsui S. Cancer outlier analysis based on mixture modeling of gene expression data. *Comput Math Methods Med*. 2013;2013:693901. <https://doi.org/10.1155/2013/693901>.

8. Lopes MB, Veríssimo A, Carrasquinha E, et al. Ensemble outlier detection and gene selection in triple-negative breast cancer data. *BMC Bioinformatics*. 2018;19:168. <https://doi.org/10.1186/s12859-018-2149-7>.
9. Rieseberg M, Kasper C, Reardon KF, Scheper T. Flow cytometry in biotechnology. *Appl Microbiol Biotechnol*. 2001;56:350–60. <https://doi.org/10.1007/s002530100673>.
10. Darzynkiewicz Z, Bedner E, Smolewski P. Flow cytometry in analysis of cell cycle and apoptosis. *Semin Hematol*. 2001;38:179–93. [https://doi.org/10.1016/S0037-1963\(01\)90051-4](https://doi.org/10.1016/S0037-1963(01)90051-4).
11. Abuhatum S, Kim K, Franzmann TM, et al. Intracellular mass density increase is accompanying but not sufficient for stiffening and growth arrest of yeast cells. *Front Phys*. 2018;6:131. <https://doi.org/10.3389/fphy.2018.00131>.
12. Park K, Millet LJ, Kim N, et al. Measurement of adherent cell mass and growth. *Proc Natl Acad Sci*. 2010;107:20691–6. <https://doi.org/10.1073/pnas.1011365107>.
13. Martínez-Martín D, Fläschner G, Gaub B, et al. Inertial picobalance reveals fast mass fluctuations in mammalian cells. *Nature*. 2017;550:500–5. <https://doi.org/10.1038/nature24288>.
14. Burg TP, Manalis SR. Suspended microchannel resonators for biomolecular detection. *Appl Phys Lett*. 2003;83:2698–700. <https://doi.org/10.1063/1.1611625>.
15. Godin M, Bryan AK, Burg TP, et al. Measuring the mass, density, and size of particles and cells using a suspended microchannel resonator. *Appl Phys Lett*. 2007;91:123121. <https://doi.org/10.1063/1.2789694>.
16. Shaw Bagnall J, Byun S, Begum S, et al. Deformability of tumor cells versus blood cells. *Sci Rep*. 2015;5:18542. <https://doi.org/10.1038/srep18542>.
17. Stevens MM, Maire CL, Chou N, et al. Drug sensitivity of single cancer cells is predicted by changes in mass accumulation rate. *Nat Biotechnol*. 2016;34:1161–7. <https://doi.org/10.1038/nbt.3697>.
18. Enoksson P, Stemme G, Stemme E. Silicon tube structures for a fluid-density sensor. *Sensors Actuators, A Phys*. 1996;54:558–62. [https://doi.org/10.1016/S0924-4247\(97\)80014-3](https://doi.org/10.1016/S0924-4247(97)80014-3).
19. Westberg D, Paul O, Andersson GI, Baltes H. CMOS-compatible device for fluid density measurements fabricated by sacrificial aluminum etching. *Sensors Actuators, A Phys*. 1999;73:243–51. [https://doi.org/10.1016/S0924-4247\(98\)00225-8](https://doi.org/10.1016/S0924-4247(98)00225-8).
20. Corman T, Enoksson P, Norén K, Stemme G. A low-pressure encapsulated resonant fluid density sensor with feedback control electronics. *Meas Sci Technol*. 2000;11:205–11. <https://doi.org/10.1088/0957-0233/11/3/306>.
21. Burg TP, Mirza AR, Milovic N, et al. Vacuum-packaged suspended microchannel resonant mass sensor for biomolecular detection. *J Microelectromechanical Syst*. 2006;15:1466–76. <https://doi.org/10.1109/JMEMS.2006.883568>.
22. von Muhlen MG, Brault ND, Knudsen SM, et al. Label-free biomarker sensing in undiluted serum with suspended microchannel resonators. *Anal Chem*. 2010;82:1905–10. <https://doi.org/10.1021/ac9027356>.
23. Miettinen T, Manalis S. Unravelling the secrets of the cell with suspended microchannel resonators. *Res Outreach*. 2019; <https://doi.org/10.32907/RO-110-4245>.
24. Etayash H, Khan MF, Kaur K, Thundat T. Microfluidic cantilever detects bacteria and measures their susceptibility to antibiotics in small confined volumes. *Nat Commun*. 2016;7:12947. <https://doi.org/10.1038/ncomms12947>.
25. Czaplewski DA, Kameoka J, Mathers R, et al. Nanofluidic channels with elliptical cross sections formed using a nonlithographic process. *Appl Phys Lett*. 2003;83:4836–8. <https://doi.org/10.1063/1.1633008>.
26. Barton RA, Ilic B, Verbridge SS, et al. Fabrication of a nano-mechanical mass sensor containing a nanofluidic channel. *Nano Lett*. 2010;10:2058–63. <https://doi.org/10.1021/nl100193g>.
27. Kim J, Song J, Kim K, et al. Hollow microtube resonators via silicon self-assembly toward subattogram mass sensing applications. *Nano Lett*. 2016;16:1537–45. <https://doi.org/10.1021/acs.nanolett.5b03703>.
28. Gagino M, Katsikis G, Olcum S, et al. Suspended nanochannel resonator arrays with piezoresistive sensors for high-throughput weighing of nanoparticles in solution. *ACS Sensors*. 2020;5:1230–8. <https://doi.org/10.1021/acssensors.0c00394>.
29. Lee J, Shen W, Payer K, et al. Toward attogram mass measurements in solution with suspended nanochannel resonators. *Nano Lett*. 2010;10:2537–42. <https://doi.org/10.1021/nl101107u>.
30. Kant R, Ziaei-Moayyed M, Howe RT. Suspended microstructures made using silicon migration. *TRANSDUCERS 2009 5th Int Conf Solid-State Sensors, Actuators Microsystems*. 2009;1091–4. <https://doi.org/10.1109/SENSOR.2009.5285949>.
31. Sato T, Mizushima I, Taniguchi S, et al. Fabrication of silicon-nothing structure by substrate engineering using the empty-space-in-silicon formation technique. *Japanese J Appl Physics, Part 1 Regul Pap Short Notes Rev Pap*. 2004;43:12-18. <https://doi.org/10.1143/JJAP.43.12>.
32. Mesbah Oskui S, Bhakta HC, Diamante G, et al. Measuring the mass, volume, and density of microgram-sized objects in fluid. *PLoS ONE*. 2017;12:e0174068. <https://doi.org/10.1371/journal.pone.0174068>.
33. Martín-Pérez A, Ramos D, Gil-Santos E, et al. Mechano-optical analysis of single cells with transparent microcapillary resonators. *ACS Sensors*. 2019;4:3325–32. <https://doi.org/10.1021/acssensors.9b02038>.
34. Ko J, Lee D, Lee BJ, et al. Micropipette resonator enabling targeted aspiration and mass measurement of single particles and cells. *ACS Sensors*. 2019;4:3275–82. <https://doi.org/10.1021/acssensors.9b01843>.
35. Maillard D, De Pastina A, Abazari AM, Villanueva LG. Avoiding transduction-induced heating in suspended microchannel resonators using piezoelectricity. *Microsystems Nanoeng*. 2021;7:34. <https://doi.org/10.1038/s41378-021-00254-1>.
36. Olcum S, Cermak N, Wasserman SC, Manalis SR. High-speed multiple-mode mass-sensing resolves dynamic nanoscale mass distributions. *Nat Commun*. 2015;6:7070. <https://doi.org/10.1038/ncomms8070>.
37. Lee J, Chunara R, Shen W, et al. Suspended microchannel resonators with piezoresistive sensors. *Lab Chip*. 2011;11:645-51. <https://doi.org/10.1039/c0lc00447b>.
38. De Pastina A, Maillard D, Özel Duygan B, et al. Single bacteria detection via piezoelectric suspended microchannel resonators. In: *23rd International Conference on Miniaturized Systems for Chemistry and Life Sciences (MicroTAS 2019)*. 2019;
39. De Pastina A, Maillard D, Villanueva LG. Fabrication of suspended microchannel resonators with integrated piezoelectric transduction. *Microelectron Eng*. 2018;192:83–7. <https://doi.org/10.1016/j.mee.2018.02.011>.
40. Vidal-Álvarez G, Marigó E, Torres F, Barniol N. Fabrication and measurement of a suspended nanochannel microbridge resonator monolithically integrated with CMOS readout circuitry. *Micromachines*. 2016;7:40. <https://doi.org/10.3390/mi7030040>.
41. Feijó Delgado F, Cermak N, Hecht VC, et al. Intracellular water exchange for measuring the dry mass, water mass and changes in chemical composition of living cells. *PLoS ONE*. 2013;8:e67590. <https://doi.org/10.1371/journal.pone.0067590>.
42. Weng Y, Delgado FF, Son S, et al. Mass sensors with mechanical traps for weighing single cells in different fluids. *Lab Chip*. 2011;11:4174–80. <https://doi.org/10.1039/c1lc20736a>.

43. Yang T, Bragheri F, Nava G, et al. A comprehensive strategy for the analysis of acoustic compressibility and optical deformability on single cells. *Sci Rep.* 2016;6:23946. <https://doi.org/10.1038/srep23946>.
44. Godin M, Delgado FF, Son S, et al. Using buoyant mass to measure the growth of single cells. *Nat Methods.* 2010;7:387–90. <https://doi.org/10.1038/nmeth.1452>.
45. Cermak N, Olcum S, Delgado FF, et al. High-throughput measurement of single-cell growth rates using serial microfluidic mass sensor arrays. *Nat Biotechnol.* 2016;34:1052–9. <https://doi.org/10.1038/nbt.3666>.
46. Calistri NL, Kimmerling RJ, Malinowski SW, et al. Microfluidic active loading of single cells enables analysis of complex clinical specimens. *Nat Commun.* 2018;9:4784. <https://doi.org/10.1038/s41467-018-07283-x>.
47. Stockslager MA, Olcum S, Knudsen SM, et al. Rapid and high-precision sizing of single particles using parallel suspended microchannel resonator arrays and deconvolution. *Rev Sci Instrum.* 2019;90:085004. <https://doi.org/10.1063/1.5100861>.
48. Son S, Grover WH, Burg TP, Manalis SR. Suspended microchannel resonators for ultralow volume universal detection. *Anal Chem.* 2008;80:4757–60. <https://doi.org/10.1021/ac800307a>
49. Jiang K, Khan F, Thomas J, et al. Thermomechanical responses of microfluidic cantilever capture DNA melting and properties of DNA premelting states using picoliters of DNA solution. *Appl Phys Lett.* 2019;114:173703. <https://doi.org/10.1063/1.5092333>.
50. Burg TP, Godin M, Knudsen SM, et al. Weighing of biomolecules, single cells and single nanoparticles in fluid. *Nature.* 2007;446:1066–9. <https://doi.org/10.1038/nature05741>.
51. Wang Y, Modena MM, Platen M, et al. Label-free measurement of amyloid elongation by suspended microchannel resonators. *Anal Chem.* 2015;87:1821–8. <https://doi.org/10.1021/ac503845f>.
52. Knudsen SM, von Muhlen MG, Manalis SR. Quantifying particle coatings using high-precision mass measurements. *Anal Chem.* 2012;84:1240–2. <https://doi.org/10.1021/ac300034r>.
53. Saha P, Duanis-Assaf T, Reches M. Fundamentals and applications of FluidFM technology in single-cell studies. *Adv Mater Interfaces.* 2020;7:1–14. <https://doi.org/10.1002/admi.202001115>.
54. Ahmad IL, Ahmad MR. Trends in characterizing single cell's stiffness properties. *Micro Nano Syst Lett.* 2014;2:8. <https://doi.org/10.1186/s40486-014-0008-5>.
55. Zhou EH, Xu F, Quek ST, Lim CT. A power-law rheology-based finite element model for single cell deformation. *Biomech Model Mechanobiol.* 2012;11:1075–84. <https://doi.org/10.1007/s10237-012-0374-y>.
56. Shaw Bagnall J, Byun S, Miyamoto DT, et al. Deformability-based cell selection with downstream immunofluorescence analysis. *Integr Biol (United Kingdom).* 2016;8:654–64. <https://doi.org/10.1039/c5ib00284b>.
57. Byun S, Hecht VC, Manalis SR. Characterizing cellular biophysical responses to stress by relating density, deformability, and size. *Biophys J.* 2015;109:1565–73. <https://doi.org/10.1016/j.bpj.2015.08.038>.
58. Byun S, Son S, Amodei D, et al. Characterizing deformability and surface friction of cancer cells. *Proc Natl Acad Sci.* 2013;110:7580–5. <https://doi.org/10.1073/pnas.1218806110>.
59. Kang JH, Miettinen TP, Chen L, et al. Noninvasive monitoring of single-cell mechanics by acoustic scattering. *Nat Methods.* 2019;16:263–9. <https://doi.org/10.1038/s41592-019-0326-x>.
60. Son S, Tzur A, Weng Y, et al. Direct observation of mammalian cell growth and size regulation. *Nat Methods.* 2012;9:910–2. <https://doi.org/10.1038/nmeth.2133>.
61. Verbridge SS, Edel JB, Stavis SM, et al. Suspended glass nanochannels coupled with microstructures for single molecule detection. *J Appl Phys.* 2005;97:124317. <https://doi.org/10.1063/1.1924888>.
62. Park J, Karsten SL, Nishida S, et al. Application of a new microcantilever biosensor resonating at the air–liquid interface for direct insulin detection and continuous monitoring of enzymatic reactions. *Lab Chip.* 2012;12:4115. <https://doi.org/10.1039/c2lc40232g>.
63. Martín-Pérez A, Ramos D, Yubero ML, et al. Hydrodynamic assisted multiparametric particle spectrometry. *Sci Rep.* 2021;11:3535. <https://doi.org/10.1038/s41598-021-82708-0>.
64. Bryan AK, Goranov A, Amon A, Manalis SR. Measurement of mass, density, and volume during the cell cycle of yeast. *Proc Natl Acad Sci.* 2010;107:999–1004. <https://doi.org/10.4132/KoreanJPathol.2012.46.4.341>.
65. Bryan AK, Hecht VC, Shen W, et al. Measuring single cell mass, volume, and density with dual suspended microchannel resonators. *Lab Chip.* 2014;14:569–76. <https://doi.org/10.1039/C3LC51022K>.
66. Kimmerling RJ, Prakadan SM, Gupta AJ, et al. Linking single-cell measurements of mass, growth rate, and gene expression. *Genome Biol.* 2018;19:207. <https://doi.org/10.1186/s13059-018-1576-0>.
67. Shalek AK, Satija R, Shuga J, et al. Single-cell RNA-seq reveals dynamic paracrine control of cellular variation. *Nature.* 2014;510:363–9. <https://doi.org/10.1038/nature13437>.
68. Kimmerling RJ, Lee Szeto G, Li JW, et al. A microfluidic platform enabling single-cell RNA-seq of multigenerational lineages. *Nat Commun.* 2016;7:10220. <https://doi.org/10.1038/ncomms10220>.

Publisher's Note Springer Nature remains neutral with regard to jurisdictional claims in published maps and institutional affiliations.